Electronic Supplementary Material (ESI) for New Journal of Chemistry.
This journal is © The Royal Society of Chemistry and the Centre National de la Recherche Scientifique 2022

An Exchange Interaction of the Antiferromagnetic Nature in Benzoato Bridged Mn(II) Chains

Romana Mičová[a], Cyril Rajnák[a*], Ján Titiš[a], Ján Moncoľ[b], Ľubor Dlháň[b], Michal Zalibera[c] and Roman Boča[a]

[a] *Department of Chemistry, Faculty of Natural Sciences, University of SS Cyril and Methodius, 917 01 Trnava, Slovakia, cyril.rajnak@ucm.sk*
[b] *Institute of Inorganic Chemistry, Slovak University of Technology, 812 37 Bratislava, Slovakia*
[c] *Institute of Physical Chemistry and Chemical Physics, Slovak University of Technology, SK-812 37 Bratislava, Slovakia*

Supplementary information (SI)

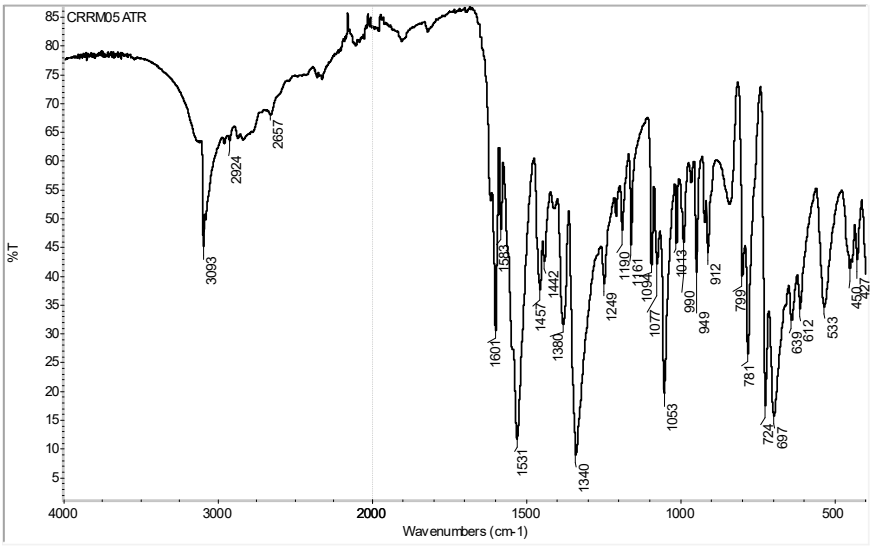

Fig. S1. FT-IR (ATR) spectrum of 1.

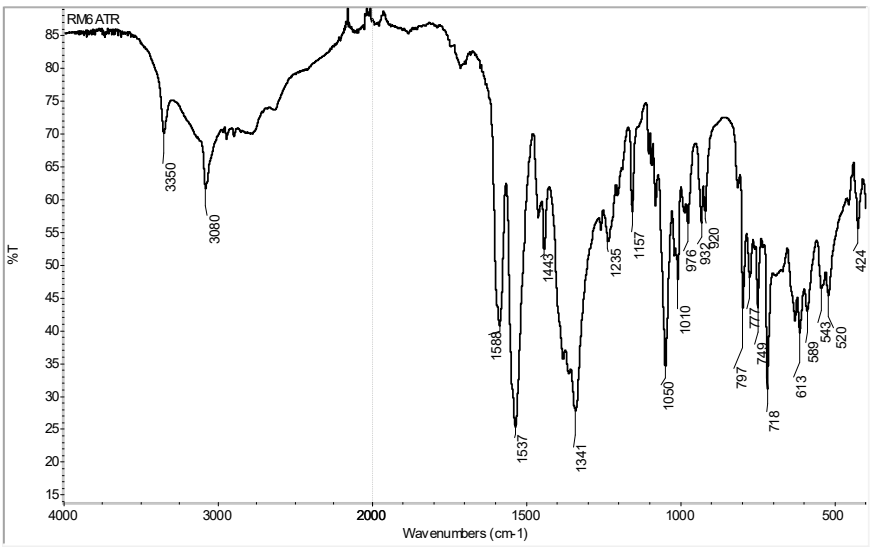

Fig. S2. FT-IR (ATR) spectrum of 2.

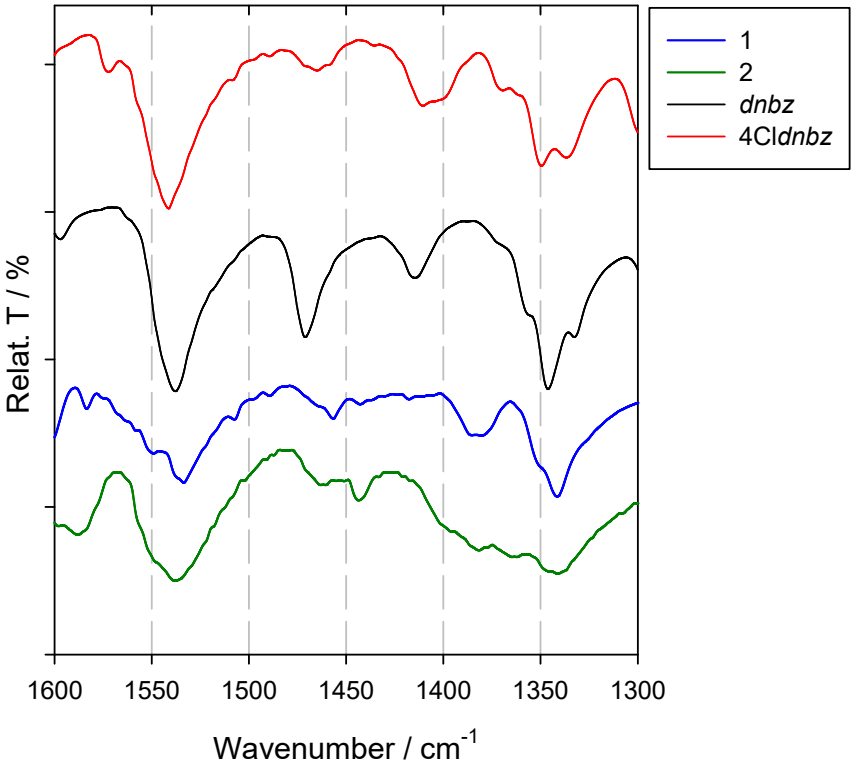

Fig. S3. The FTIR-ATR spectrum cutout of **1** and **2**.

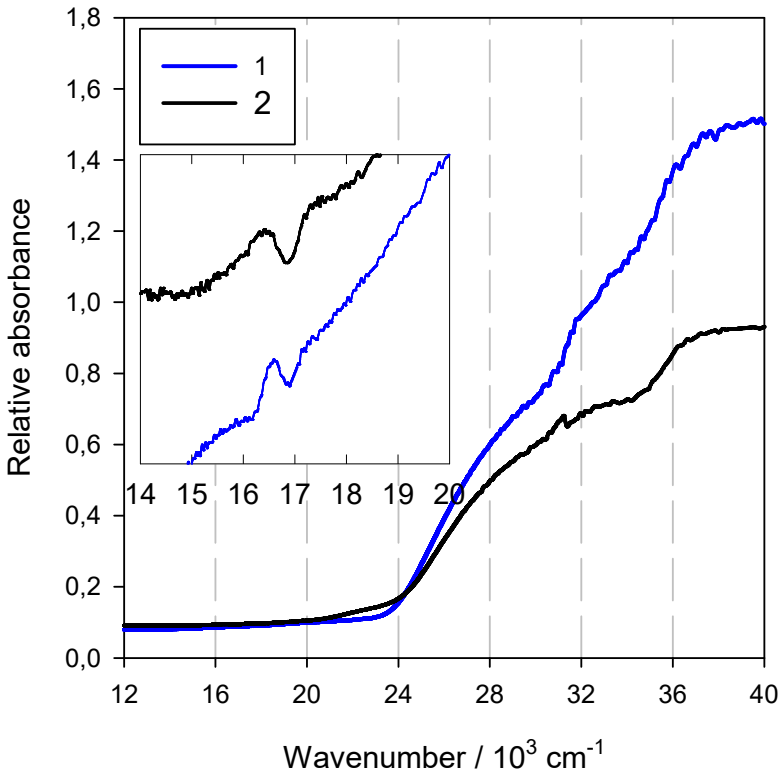

Figure S4. Electronic specra of 1-2.

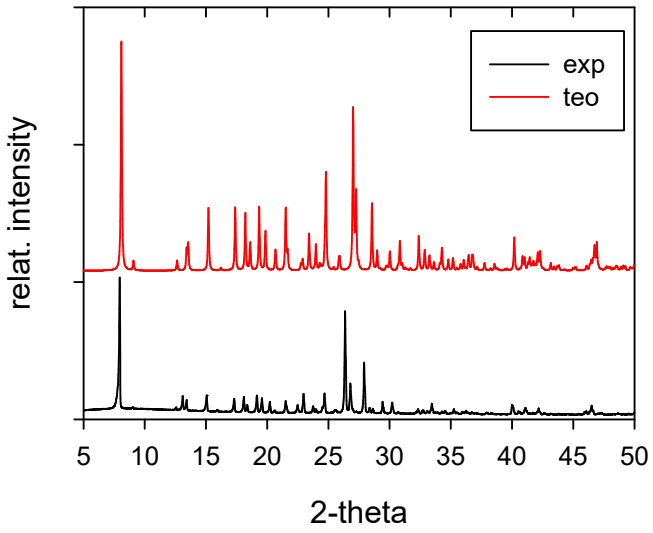

Figure S5. Calculated powder diffraction pattern for **1** from cif.file (red), and recorded pattern at Cu, λ = 1.54060 Å (black).

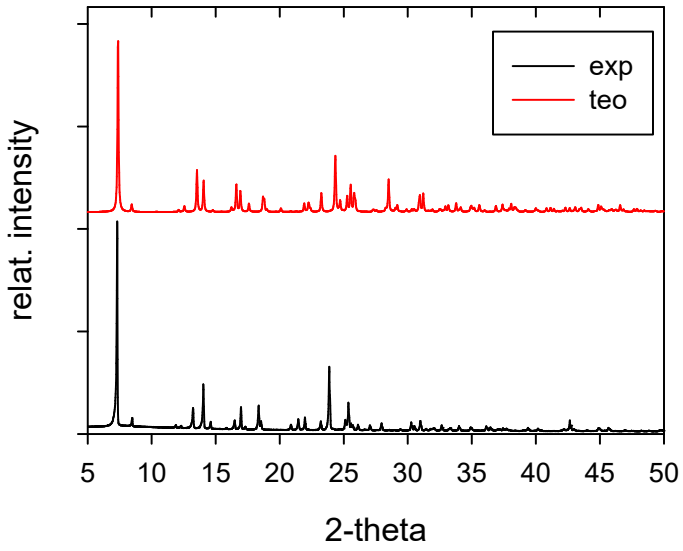

Figure S6. Calculated powder diffraction pattern for **2** from cif.file (red), and recorded pattern at Cu, λ = 1.54060 Å (black).

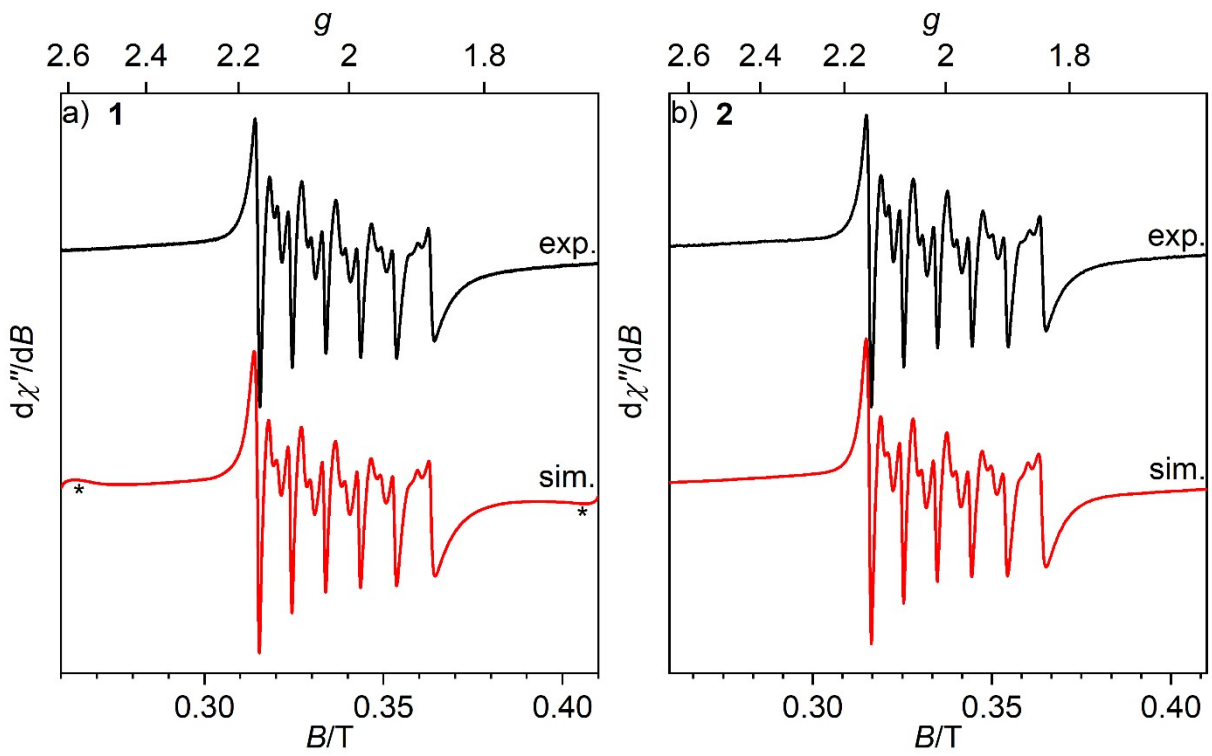

Figure S7. X-band (9.5 GHz) EPR spectra of a) **1** and b) **2** in frozen methanol glass at 77 K (black lines). The spectral simulations (red lines) were calculated using spin Hamiltonian $\hat{H}/hc = g\mu_B B\hat{S}_z + D[\hat{S}_z + S(S+1)/3] + E(\hat{S}_x^2 - \hat{S}_x^2) + A\hat{S}_z\hat{I}_z$

with paramaters:

a) $g = 2.004$, $A(^{55}\text{Mn}) = 90 \times 10^{-4}\ \text{cm}^{-1}$, $|D| = 185 \times 10^{-4}\ \text{cm}^{-1}$, $|E| = 50 \times 10^{-4}\ \text{cm}^{-1}$. Line broadening model assumed a broad Gaussian distribution of ZFS parameters [1] with full width at half maximum (FWHM) $D_{\text{FWHM}} = 180 \times 10^{-4}\ \text{cm}^{-1}$, $E_{\text{FWHM}} = 40 \times 10^{-4}\ \text{cm}^{-1}$. * mark simulation artifacts due to the trimmed spectral range

b) $g = 2.001$, $A(^{55}\text{Mn}) = 90 \times 10^{-4}\ \text{cm}^{-1}$, $|D| = 202 \times 10^{-4}\ \text{cm}^{-1}$, $|E| = 50 \times 10^{-4}\ \text{cm}^{-1}$. Line broadening model assumed a broad Gaussian distribution of ZFS parameters $D_{\text{FWHM}} = 140 \times 10^{-4}\ \text{cm}^{-1}$, $E_{\text{FWHM}} = 38 \times 10^{-4}\ \text{cm}^{-1}$

Table S1. Structural features of 1D polymeric chains with $\{MnO_6N_1\}$ chromophore.

Complex	CCDC No	Chromophore	SHAPE agreement factor[a]					Preferred geometry	Ref
			5bpy	HP	HPY	C0C	CTPR		
$[Mn^{II}(L^1)(L^2)_4]_n$	1992055	$\{MnO_6N\}$	0.805	33.582	24.222	5.630	4.305	5bpy	tw
$[Mn^{II}(L^1)(L^3)_4]_n$	1992057	$\{MnO_6N\}$	1.157	34.674	24.331	4.780	3.376	5bpy	tw
$[Mn^{II}HL\cdot(AcO)\cdot 2\ C_2H_5OH]$	634809	$\{MnO_6N\}$	0.788	32.623	24.076	7.383	5.834	5bpy	[2]
$[Mn^{II}(H_2L)(NO_3)_2(CH_3OH)]\cdot CH_3OH$	1548163	$\{MnO_6N\}$	2.480	30.177	22.383	4.230	3.183	5bpy	[3]

[a] Program SHAPE [4]; HL = (*Z*)-2-hydroxy-*N'*-(2-oxoindolin-3-ylidene)benzohydrazide; H_2L = (*E*)-3-hydroxy-*N'*-(1-(2-oxo-2H-chromen-3-yl)ethylidene)-2-naphthohydrazide; HP = Heptagon, HPY = Hexagonal pyramid, C0C = Capped octahedron, CTPR = Capped trigonal prism

Table S2. Selected bond lengths (Å) in complexes **1**–**2**.

1					
Mn1–O1	2.314(1)	Mn1–O2	2.194(1)	Mn1–O3^{iv}	2.310(1)
Mn1–O1^{iii}	2.314(1)	Mn1–O2^{iii}	2.194(1)	Mn1–O3^{v}	2.310(1)
Mn1–N1	2.279(2)				
2					
Mn1–O1	2.308(2)	Mn1–O2	2.298(2)	Mn1–O3	2.153(2)
Mn1–O4^{i}	2.318(2)	Mn1–O9	2.154(2)	Mn1–O10^{vi}	2.312(2)
Mn1–N1	2.305(2)				

Symmetry code: (i) 1–*x*, 1–*y*, 1–*z*; (iii) 1–*x*, *y*, 1/2–*z*; (iv) 1–*x*, –*y*, 1–*z*; (v) *x*, –*y*, –1/2–*z*; (vi) –*x*, 1–*y*, 1–*z*.

Table S3. Selected bond angles (°) in chromophore of 1-2.

1	(°)		(°)
O1-Mn1-O1^1	141.18	O2-Mn1-N1	88.89
O2^1-Mn1-O1	96.77	O2^1-Mn1-N1	88.89
O2-Mn1-O1^1	96.77	O3^3-Mn1-O1^1	143.48
O2^1-Mn1-O1^1	82.49	O3^3-Mn1-O1	74.27
O2-Mn1-O1	82.49	O3^2-Mn1-O1^1	74.27
O2-Mn1-O2^1	177.79	O3^2-Mn1-O3^3	143.51
O2^1-Mn1-O3^2	96.97	N1-Mn1-O1	70.59
O2^1-Mn1-O3^3	84.81	N1-Mn1-O1^1	70.59
O2-Mn1-O3^2	84.81	N1-Mn1-O3^3	143.25
O2-Mn1-O3^3	96.98	N1-Mn1-O3^2	143.25
2			
O1-Mn1-O4^1	141.21	O3-Mn1-O10^2	82.26
O2^1-Mn1-O10^2	76.87	O3-Mn1-N1	87.96
O2-Mn1-O1	140.53	O9-Mn1-O1	84.73
O2^1-Mn1-O4^1	76.75	O9-Mn1-O2	93.39
O2-Mn1-O10^2	141.34	O9-Mn1-O4^1	82.05
O2-Mn1-N1	70.52	O9-Mn1-O10^2	101.45
O3-Mn1-O1	95.15	O9-Mn1-N1	88.39
O3-Mn1-O2	84.24	O10^2-Mn1-O4^1	70.36
O3-Mn1-O4^1	100.31	N1-Mn1-O1	70.03
O3-Mn1-O9	176.15	N1-Mn1-O4^1	145.23
		N1-Mn1-O10^2	144.41

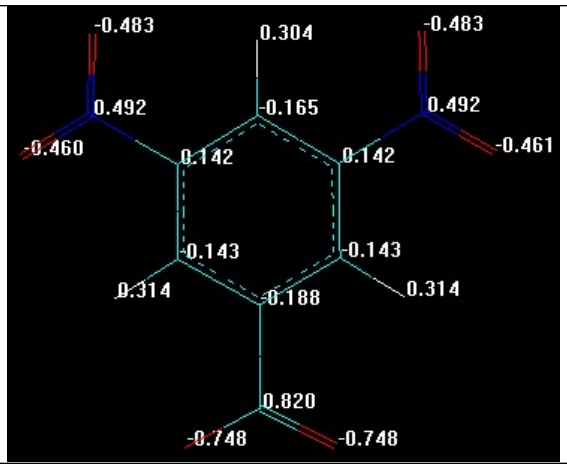

L^2 = 3,5-dinitrobenzoate
E_{tot} = –827.079, E_{corr}(MP2) = –2.371 a.u.

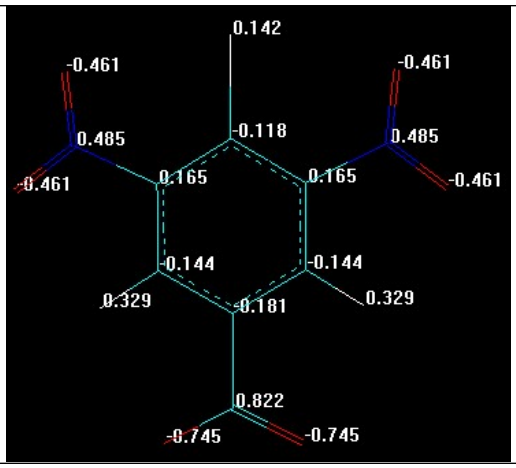

L^3 = 4-chloro-3,5-dinitrobenzoate
E_{tot} = –1286.093, E_{corr}(MP2) = –2.524 a.u.

Figure S8. The charge population for anionic ligands calculated at the HF-MP2/6-31G* level of theory (for L^2 and L^3, the partial charges on the oxygen atoms of the carboxyl group are practically the same).

Table S4. Bond valence sum analysis for complex **1**.

	Mn-L(r_{ij})	R_0(II)	R_0(III)	R_0(IV)	s_{ij}(II)	s_{ij}(III)	s_{ij}(IV)
Mn1–O1	2.314	1.765	1.732	1.750	0.227	0.207	0.218
Mn1–O1^{iii}	2.314	1.765	1.732	1.750	0.227	0.207	0.218
Mn1–O2	2.194	1.765	1.732	1.750	0.314	0.287	0.301
Mn1–O2^{iii}	2.194	1.765	1.732	1.750	0.314	0.287	0.301
Mn1–O3^{iv}	2.310	1.765	1.732	1.750	0.229	0.210	0.220
Mn1–O3^{v}	2.310	1.765	1.732	1.750	0.229	0.210	0.220
Mn1–N1	2.279	1.849	1.837	1.822	0.313	0.303	0.291
***V*(Mn)=$\sum s_{ij}$**					**1.852**	**1.711**	**1.769**

$s_{ij} = \exp\left[\left(R_0 - r_{ij}\right)/0.37\right]$, R_0 - empirical parameter [5].

Table S5. Bond valence sum analysis for complex **2**.

	Mn-L(r_{ij})	R_0(II)	R_0(III)	R_0(IV)	s_{ij}(II)	s_{ij}(III)	s_{ij}(IV)
Mn1–O1	2.308	1.765	1.732	1.750	0.230	0.211	0.221
Mn1–O2	2.298	1.765	1.732	1.750	0.237	0.217	0.227
Mn1–O3	2.153	1.765	1.732	1.750	0.350	0.321	0.336
Mn1–O4^{i}	2.318	1.765	1.732	1.750	0.224	0.205	0.215
Mn1–O9	2.154	1.765	1.732	1.750	0.349	0.320	0.336
Mn1–O10^{vi}	2.312	1.765	1.732	1.750	0.228	0.209	0.219
Mn1–N1	2.305	1.849	1.837	1.822	0.292	0.282	0.271
***V*(Mn)=$\sum s_{ij}$**					**1.911**	**1.764**	**1.826**

$s_{ij} = \exp\left[\left(R_0 - r_{ij}\right)/0.37\right]$, R_0 - empirical parameter [5].

LOBA for mononuclear complex unit of **1**

Oxidation state of atom 1(Mn) : 2
Oxidation state of atom 2(O) : -2
Oxidation state of atom 3(H) : 1
Oxidation state of atom 4(N) : -3
Oxidation state of atom 5(C) : 0
Oxidation state of atom 6(H) : 1
Oxidation state of atom 7(H) : 1
Oxidation state of atom 8(C) : 4
Oxidation state of atom 9(C) : 2
Oxidation state of atom 10(H) : 1
Oxidation state of atom 11(C) : 2
Oxidation state of atom 12(H) : 1
Oxidation state of atom 13(O) : -2
Oxidation state of atom 14(H) : 1
Oxidation state of atom 15(C) : 0
Oxidation state of atom 16(H) : 1
Oxidation state of atom 17(H) : 1
Oxidation state of atom 18(C) : 4
Oxidation state of atom 19(C) : 2
Oxidation state of atom 20(H) : 1
Oxidation state of atom 21(C) : 4
Oxidation state of atom 22(C) : 4
Oxidation state of atom 23(C) : 2
Oxidation state of atom 24(H) : 1
Oxidation state of atom 25(C) : 4
Oxidation state of atom 26(C) : 2
Oxidation state of atom 27(H) : 1
Oxidation state of atom 28(C) : 4
Oxidation state of atom 29(C) : 2
Oxidation state of atom 30(H) : 1
Oxidation state of atom 31(N) : 3
Oxidation state of atom 32(N) : 3
Oxidation state of atom 33(O) : -2
Oxidation state of atom 34(O) : -2
Oxidation state of atom 35(O) : -2
Oxidation state of atom 36(O) : -2
Oxidation state of atom 37(O) : -2
Oxidation state of atom 38(O) : -2
Oxidation state of atom 39(O) : -2
Oxidation state of atom 40(O) : -2
Oxidation state of atom 41(O) : -2
Oxidation state of atom 42(O) : -2
Oxidation state of atom 43(O) : -2
Oxidation state of atom 44(O) : -2
Oxidation state of atom 45(N) : 3
Oxidation state of atom 46(N) : 3
Oxidation state of atom 47(C) : 4
Oxidation state of atom 48(C) : 4
Oxidation state of atom 49(C) : 2
Oxidation state of atom 50(H) : 1
Oxidation state of atom 51(C) : 4
Oxidation state of atom 52(C) : 2
Oxidation state of atom 53(H) : 1
Oxidation state of atom 54(C) : 4
Oxidation state of atom 55(C) : 2
Oxidation state of atom 56(H) : 1
Oxidation state of atom 57(O) : -2
Oxidation state of atom 58(O) : -2
Oxidation state of atom 59(H) : 1
Oxidation state of atom 60(H) : 1
Oxidation state of atom 61(H) : 1
Oxidation state of atom 62(H) : 1
Oxidation state of the fragment: -2 – sum of the ligand fragments

Rereferences for SI

[1] R. C. Hadley, D. M. Gagnon, A. Ozarowski, R. D. Britt, E. M. Nolan. *Inorg. Chem.* 2019, *58*, 13578–13590.

[2] X. Zhong, H.-L- Wei, W.-S. Liu, D.-Q. Wang, X. Wang. *Bioorg. Med. Chem. Lett.,* 2007, 17, 3774.

[3] R. Bikas, H.-F. Bonab, N. Noshiranzadeh, M. Aygun, M. Emami, T. Lis. *J. Coord. Chem,* 2018, 71*,* 1127.

[4] M. Llunell, D. Casanova, J. Cirera, P. Alemany, S. Alvarez. Program SHAPE, Ver. 2.1. University of Barcelona. Note: the program assumes a spherical distribution of the ligands in ideal reference polygons or polyhedra, 2013.

[5] Brown, I. D.; Altermatt, D. Bond-Valence Parameters Obtained from a Systematic Analysis of the Inorganic Crystal Structure Database. *Acta Crystallogr. B.* 1985, B41, 244.